

"Faster" Could be "Slower": Uncovering the Salient Characteristics of Slow-light Guided Signals with the Finite-Difference-Time-Domain (FDTD) Method

Stavroula Foteinopoulou

Department of Electrical and Computer Engineering
University of New Mexico, Albuquerque, NM 87131, USA
sfoteino@unm.edu

Abstract — Slow-light mesophotonic waveguides have gained increasing interest in the recent years because of their catalyzing potential to transform applications relying on all-optical signal manipulation or enhanced light-matter interactions. The quests in this area have been targeting waveguide platforms with a giant group velocity index as determined by modal type of analyses in frequency domain. We show here that these efforts with frequency-domain methods have entirely missed on important mode features which are nevertheless crucial in practically effecting an ultra-slow guided pulsed signal with a large time delay. We utilize first-principle electromagnetic (EM) simulations in time-domain and show that contrary to conventional wisdom, the group-index by itself is not in general a good measure of the slow-down factor for a pulsed light signal propagating within the waveguide. We present a counterexample comparing two modes which demonstrates that the “faster” mode, the one with the lower group index, is the one that leads to larger effective time delays. The time-domain analysis in this counter-example uncovers a new figure of merit for practical slow-light platforms which indicates that along with a near-zero group velocity, a relatively low group-velocity dispersion value is simultaneously required.

Index Terms — Finite Difference Time Domain (FDTD) method, group index, group velocity, group velocity dispersion, left-handed materials, negative-index media, slow light, wave dispersion.

I. INTRODUCTION

Electromagnetic (EM) waveguiding platforms across the board have been predominantly studied in a frequency-domain framework for modal responses. In such framework, the modal behavior for the system is sought for a certain frequency, ω , and wavevector, \mathbf{k} . Such modal response can be calculated analytically for simple planar geometries, such as in dielectric slab [1], metallic [2-4], metal-slot [2,5], and negative-refractive-index waveguides [6] as well as for their heterostructures [7]. As the guiding structures however become more

complicated, as for example in metallic periodically corrugated waveguides [8], metal/dielectric-strip waveguides [9] or all-dielectric designer surface plasmon waveguides [10-13], numerical approaches are needed to determine both the wave dispersion and spatial field profiles for the modes supported by the guiding system. One widely adopted example of such numerical approaches is the Finite-Difference-Frequency-Domain (FDFD) method [10,14-16].

While important information for a system’s response to incoming EM waves can be obtained with these frequency-domain methods, a complete picture for the dynamic evolution of the propagating wave cannot actually be trivially deduced. Realistic source excitations are neither a perfect plane wave nor are they perfectly monochromatic even at continuous wave (CW) excitation. A framework for time-domain analysis is certainly highly desirable, especially for systems where the dynamic evolution of the guided wave is key to their operational principle. One such example is waveguides that support ultra-slow light waves [17] which have been realized in plasmonic-based systems [9, 18], in platforms based on negative-refractive-index metamaterials [7, 19-21], in photonic-crystal waveguides [22-24], as well as in certain atomically-thin materials with a phonon-polariton photonic response [25].

In this paper, we show that a time-dependent framework is key to obtaining understanding and uncovering design principles for slow-light platforms for practical applications. In principle, the system’s time-domain response can be constructed from frequency-domain methods with the use of rigorous-modal matching analysis [26]. Actually, using this composite detailed analysis, He et al. [26] showed that a wave-packet in a tapered metamaterial waveguide gets back-reflected rather than attaining the “trapped rainbow” effect [21] which was hypothesized based on a purely frequency-domain analysis. However, the process followed by Ref. [26] can get quickly elaborate as structures or EM-wave launch geometries get more complicated and may require approximations that limit the range of validity. A brute-force, ab-initio method for

time-domain analysis is highly attractive. Free from any assumptions for simplifications, a highly popular widely used method for analysis in the time-domain is the Finite-Difference-Time-Domain (FDTD) method [27], which allows modeling of actual experimental set-ups.

In the following, we demonstrate why FDTD is highly suited for designing slow-light waveguides, uncovering salient mode characteristics that were missed with modal frequency-domain analyses. In particular, this paper is organized as follows. In Sec. II, we present the paradigm system that will be analyzed in two variations; these will serve as the counter-example showing that it is the system with the higher group velocity practically yielding the larger time delay for a guided pulsed signal. In Sec. III we analyze these designs in frequency-domain determining a prediction for their behavior as slow-light waveguides. In Sec. VI, we discuss the methodology to calculate appropriately the effective time delay and speed of a pulsed signal in the FDTD method. In Sec. V, we apply this methodology in the two paradigm system variations and extract an additional design principle that has been hitherto missed from standard modal dispersion analysis. Finally, we present our conclusions in Sec. VI.

II. THE SLOW-LIGHT BI-WAVEGUIDE PARADIGM SYSTEM

We use the paradigm system of Ref. [7] as a counter-example to show that the frequency-domain predictions for a near-zero group velocity in two waveguide designs do not end-up yielding ultra-slow guided light in time-domain for both cases. This paradigm system is a bi-waveguide comprising a regular dielectric slab waveguide [1], i.e., a positive-index-medium (PIM) waveguide, and a slab waveguide made from a negative-index-medium (NIM) [see Fig. 1]. In the PIM waveguide, the guided mode has the Poynting vector \mathbf{S} , parallel to the direction of phase propagation, as given by the wavevector \mathbf{k} . Conversely, in the NIM waveguide the Poynting vector \mathbf{S} , is anti-parallel to the direction of phase propagation [6]. Outside the waveguide the EM energy decays exponentially (evanescent waves). The evanescent tails of the guided mode do carry some energy along the $+x$ direction, but this can be neglected in this case as the main waveguides have a width of about three times the free space wavelength.

As we also depict in Fig. 1, the phase (wave vector) direction is common in both constituent waveguides, as imposed by Maxwell's equations requiring continuity of the parallel component of the wave-vector across the waveguide interfaces. Then, it follows from the respective Poynting vector directions that the EM energy would have a disposition to propagate in opposite directions in each sub-waveguide if the waveguides were independent. Because of this competition in the direction of energy propagation in each of the sub-waveguides,

Ref. [19] envisioned the composite PIM-NIM bi-waveguide to possess nearly-frozen light modes. These manifest themselves in the waveguide dispersion relation, $\omega(k_x)$, with near-zero group velocity, i.e., $\partial\omega/\partial k_x=0$. Guided modes with near-zero group velocity can be found for a range of parameters in this system. An additional benefit of the PIM-NIM bi-waveguide is that it is also favorable for monomodal response [28].

(a) Bi-waveguide A, $d_A=4.54 \mu\text{m}$

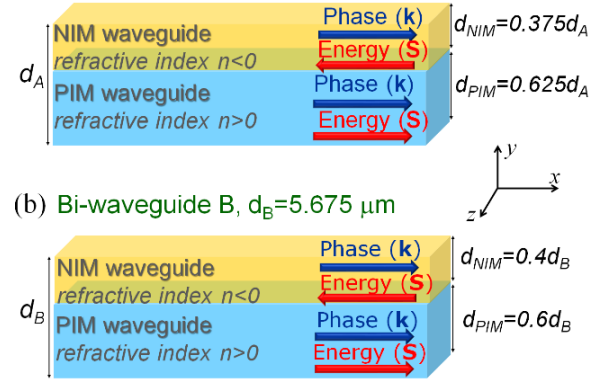


Fig. 1. The slow-light bi-waveguide paradigm system comprising a positive-index-medium (PIM) waveguide and a negative-index-medium (NIM) waveguide. Two cases, depicted in (a) and (b), have been chosen in order to showcase two near-zero group velocity examples but with distinctly different effective responses to an input EM signal. In each case, the widths for the individual PIM, NIM waveguides as well as the total width of the bi-waveguide are indicated.

We focus now our attention on two particular bi-waveguide designs A and B, in order to demonstrate how the FDTD method distinguishes the behavior between two modes which are both identified as slow-light modes with a modal analysis. Both bi-waveguide designs comprise the same materials: a permittivity of $\epsilon=4.0$ for the PIM, and the Veselago dispersive material [29] for the NIM with a plasma frequency of $\omega_p=2\pi\cdot 308\cdot 10^{12}$ rad/s. The chosen waveguide widths however for each sub-waveguide, d_{NIM} and d_{PIM} , are different and result in a different total width for the bi-waveguide. In the following, we designate the total bi-waveguide width as d_A , and d_B , for design A and design B respectively (see Fig. 1 for their values). We note, the paradigm system is idealized, e.g., actual metamaterials do not follow the Veselago medium response. The purpose of using this idealized paradigm is to understand how features in the frequency-domain modal response effect behaviors in time-domain. This link is what has not been hitherto well understood. This understanding is however of utmost importance to design practical systems that guide ultra-slow EM pulses.

In the following section we present and compare the predictive response of the two paradigm designs based on a modal frequency-domain analysis.

III. BI-WAVEGUIDE DESIGNS A AND B: PROPERTIES IN FREQUENCY DOMAIN

The simple planar geometry of the bi-waveguide system allows calculating analytically the dispersion relation of the guided mode, $\omega(k_x)$, i.e., the relation between the frequency and the wave vector along the guide direction. This is done by considering a guided wave solution in the PIM, and NIM region, and evanescent tails outside the waveguide; the wave dispersion is then determined by applying the EM boundary conditions for the continuity of the tangential components of the electric and magnetic field (see Ref. [7] for details). This is depicted in Fig. 2 (a). Both frequency and wave vector are represented in dimensionless units [see caption of Fig. 2]. The dimensionless scaled wave vector along the guide direction, β , is also known as modal index [30]. We observe that a single guided-mode is present for each design in this frequency range. We recognize that for a range of modal index values the dispersion flattens for both waveguide designs. We designate this dispersion region with a yellow shading in Fig. 2 (a) and show it magnified in Fig. 2 (b) for both waveguide designs.

This nearly-flat dispersion region signifies a near-zero group velocity magnitude, v_g , and conversely a very large group index (absolute value), $|n_g|$, since:

$$v_g = \left| \frac{\partial \omega}{\partial k_x} \right| = \frac{c}{|n_g|}, \quad (1)$$

where ω is the guided wave cyclic frequency, k_x , is the wavevector along the guiding direction and c is the speed of light. Equation (1) implies that a large group-index magnitude leads to a large light slow-down factor for the guided wave. For the case of design B, the dispersion band has a negative slope in a range of modal index values, and yields a negative group index, n_g . In Fig. 2 (c) the group index (absolute value) is plotted, but we use a dashed line, instead of a solid line, to designate the range for which the group index is negative (see also Ref. [31]).

We also mark in Fig. 2 (c) certain modes of interest for waveguide A and waveguide B. First, we make note of modes SLA and SLB, shown with a blue box and a red box, respectively. What is interesting about these two modes is that both have large group index (absolute values); so in principle both look like good candidate modes for slow-light guiding. Mode SLA has a group index of ~ 100 and mode SLB's group index is even higher, ~ 2000 . So, if one was to think of a good slow-light waveguide design the obvious choice from such frequency domain analysis would be design B operating

at mode SLB. We will see however with the time-domain analysis in the following that this is not true; we will find that it is actually design A at mode SLA that makes a good slow-light waveguide. For this purpose, we need to analyze the signal propagation along the waveguide for both slow-light waveguide candidates in time-domain. Before doing so, we present in the following the details of the numerical determination of the signal propagation speed for a more general case of a moderate group index. We choose mode LB of design B, that we have designated with a brown square in Fig. 2 (c).

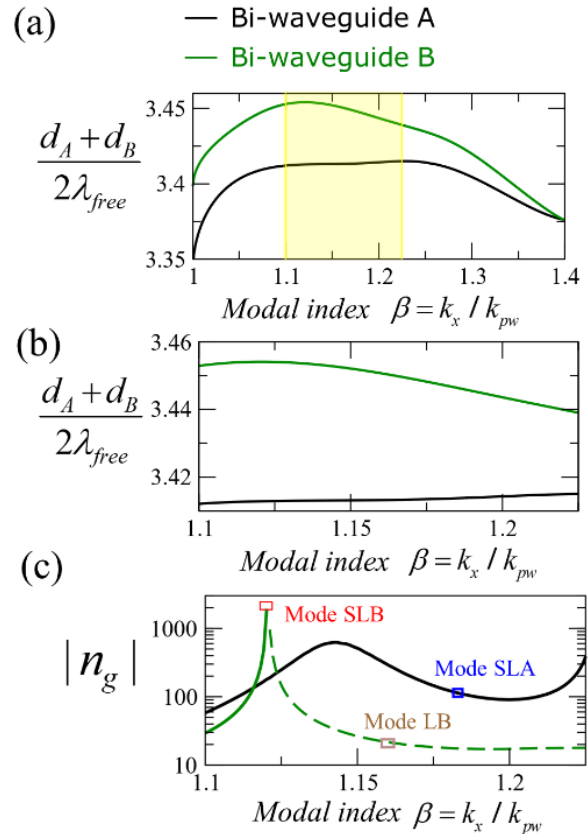


Fig. 2. (a) The wave dispersion for the two bi-waveguide designs, A and B of Fig. 1. Both the frequency and the wavevector along the guiding direction, x , are represented in dimensionless units; the former by multiplying the inverse of the free-space wavelength, λ_{free} , with the average width of the two waveguide designs and the latter by dividing with the free-space plane-wave wavevector, k_{pw} , to give β , which is known as the modal index [30]. The shaded area designates a region of nearly-flat dispersion for both designs. (b) Zoom of the shaded region of (a). (c) Magnitude of the group index, $|n_g|$, (logarithmic scale) versus the modal index, β , for the two waveguide cases [dashed lines indicate regions with $n_g < 0$]. The three modes that are labeled (SLA, SLB and LB) will be analyzed further.

IV. SIGNAL PROPAGATION SPEED IN FDTD: CALCULATION METHOD

In the FDTD framework, a numerical experiment with an Otto set-up [7, 10-11, 32] can be implemented for the determination of the propagating signal's speed. The Otto set-up yields an evanescent wave that further excites the guided mode in the bi-waveguide system. The right-angle prism of the Otto configuration, lies above the bi-waveguide system of Fig. 1, with its hypotenuse along the x -direction; it so fixes the modal index to $\beta_0 = n_{\text{prism}} \sin(45^\circ)$ since EM boundary condition require the wavevector along the x -direction to be conserved. Therefore, an EM wave launched from the left-side of a prism with $\beta_0 = \beta_{\text{LB}}$ would couple to mode LB with a wavevector along the $+x$ -direction. As mode LB has a negative group index as determined in Sec. III, the composite waveguide mode is expected to be a backward type of mode [10-11, 33]. This means the EM energy of the composite guided wave will propagate opposite to its wavevector, i.e., in the $-x$ direction. Indeed, we observe in the FDTD calculations that despite the different Poynting vector directions in the NIM and PIM sub-waveguide parts, in both of them the pulsed signal propagates in the direction predicted by the dispersion-band slope direction, i.e., in the $-x$ direction for mode LB (see also Refs. [7] and [31]).

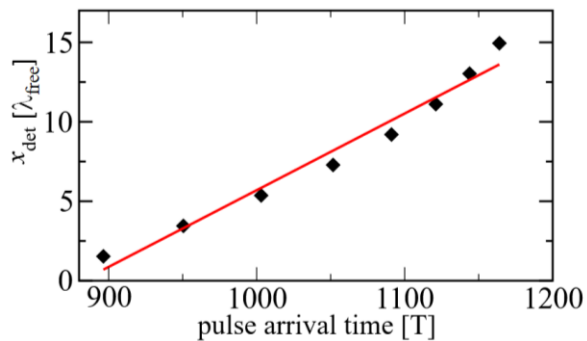


Fig. 3. FDTD results (filled diamonds) for the detector position, x_{det} , versus the arrival time of the pulsed signal at this detector for mode LB. The detector position is scaled with the free space wavelength, λ_{free} , while the pulse arrival time is scaled with the wave period T of the central frequency of the input EM pulse (filled diamonds). The red solid line represents a linear fit on the FDTD data.

To avoid any interference that would come from the reflected signal at the waveguide edges, the FDTD simulation set-up has the bi-waveguide terminated with suitable absorbers in both sides [see Ref. 7]. Different detectors are placed at various distances, x_{det} , from the left-side of the prism, to span different positions along the $-x$ direction. Each detector extends across the entire bi-waveguide width in the y -direction. For each of the

detectors, each positioned at different x_{det} , the Poynting vector along the guide direction, S_x , is recorded at each time step for all spatial grid points in the y -extend of the detector. As the waveguide system is strongly dispersive it is not appropriate to monitor the peak of the pulse in order to determine its arrival time. To determine the EM signal's speed in the FDTD implementation of the bi-waveguide system, we follow a similar approach to that introduced by Peatross et al. in Ref. [34].

In particular, we calculate the arrival time, t_{arr} , at a detector at position x_{det} from:

$$t_{\text{arr}}(x_{\text{det}}) = \frac{\int_0^{t_{\text{sim}}} t \left(\int_0^{d_B} S_x(x_{\text{det}}, y, t) dy \right) dt}{\int_0^{t_{\text{sim}}} \left(\int_0^{d_B} S_x(x_{\text{det}}, y, t) dy \right) dt}, \quad (2)$$

with d_B being the bi-waveguides B width across the y -direction (see schematics in Fig. 1). The FDTD simulation is terminated at t_{sim} at which time the signal strength should be at least three magnitudes lower than its peak value (the lower the more accurate the calculation). We show the results calculated from Eq. (2) with the FDTD method in Fig. 3. The numerical FDTD data can be fitted with a linear fit (red-solid line in the figure). From, the slope of the $x_{\text{det}}(t_{\text{arr}})$ fit line we determine $|n_g|$ for mode LB to be 20.7 which agrees excellently with the value determined from the frequency-domain analysis which is 21.7 [see Fig. 2 (c)]. So, we did not find any surprises for the case of mode LB and both frequency and time domain analysis agree on the propagating properties of the guided pulsed signal. Whether this holds to be true for the ultra-slow guided modes, namely modes SLA and SLB in Fig. 2 (c), we explore in the following section.

V. SIGNAL PROPAGATION SPEED OF MODES AT FLAT WAVE DISPERSION: FREQUENCY-DOMAIN VERSUS TIME-DOMAIN PREDICTIONS

Now we follow the process of Sec. IV in the FDTD simulations for mode SLA of waveguide design A and mode SLB of waveguide design B. Both correspond to regions of flat guided wave dispersion, $\omega(k_x)$. For design A, we obtain an effective slow down factor of ~ 300 which is actually quite higher than the frequency-domain prediction of ~ 100 . The FDTD result for the SLB waveguide is even more cumbersome. We find that the effective slow down factor varies with the distance from the prism edge between the values ~ 10 and 40 which is about two orders of magnitude lower than the frequency-domain prediction of ~ 2000 . We discuss below where this huge discrepancy between modal analysis and time-domain observations for mode SLB is coming from.

The input EM wave, has a Gaussian beam waist, which implies a spread $\Delta\beta$ around the β_0 value

corresponding to a certain mode. All observed guided waves, around LB, SLA and SLB modes are subject to the influence of the modal index spread, $\Delta\beta$, which introduces additional modes in the vicinity of the respective intended modes, e.g., LB, SLA or SLB. The case of mode SLB, is especially peculiar however when compared to the case of modes LB and SLA. The difference between mode SLB and modes LB and SLA is that the group index, n_g changes so much around mode SLB with modal index, β to the point that it goes from positive to negative.

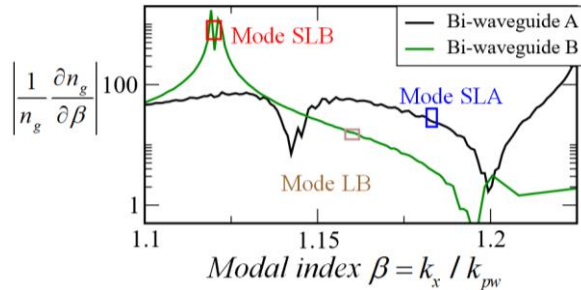


Fig. 4. Comparison of the relative group index variation with the modal index (absolute value), versus the modal index β for the different modes.

It appears there is a correlation between consistency of modal and time-domain analysis and the variation of the group index n_g with the modal index, β . We therefore plot in Fig. 4, the relative group index variation with the modal index (absolute value), i.e., $|\partial n_g / \partial \beta| / |n_g|$ versus the modal index β for both the bi-waveguide designs. This quantity is calculated from the dispersion relations of Fig. 2 (b). We also designate the modes LB, SLA and SLB that we have discussed above. Figure 4 confirms that the lower the value of this quantity the better the agreement between frequency-domain predictions and time-domain calculations for the effective guided-mode slow-down factor. In other words, the quantity $|\partial n_g / \partial \beta| / |n_g|$ can serve as a figure of merit (FOM) for slow-light waveguides, with lower values indicating a better performance. It can be shown that if $|n_g| \gg \beta$, which is typically the case for modes identified as slow modes in a modal analysis that:

$$FOM = \left| \frac{1}{n_g} \frac{\partial n_g}{\partial \beta} \right| \cong |GVD(\omega_0)| \cdot v_g^2 \cdot \frac{\omega_0}{c}, \quad (3)$$

with ω_0 being the frequency of the corresponding mode and GVD the group velocity dispersion at that frequency. Equation (3) implies that along with a near-zero group velocity a relatively small GVD value is simultaneously required to practically achieve high effective slow-down factors.

VI. CONCLUSION

Our analysis here suggests that the Finite-Difference-Time Domain (FDTD) method gives a more complete picture for the system's response in a particular experimental set-up. Thus, the FDTD method is more suitable to characterize practical slow-light systems in comparison with modal methods in the frequency domain. The FDTD analysis on a paradigm system uncovered a figure of merit for design guidance of slow-light platforms. The latter stresses on the importance of an as low as possible GVD value along with a near-zero group velocity to practically achieve slow-light propagation.

REFERENCES

- [1] D. Marcuse, *Theory of Dielectric Optical Waveguides*. 2nd edition, Elsevier Inc., 1991.
- [2] E. N. Economou, "Surface plasmons in thin films," *Phys. Rev.*, vol. 182, pp. 539-554, 1969.
- [3] J. A. Dionne, et al., "Planar metal plasmon waveguides: frequency-dependent dispersion, propagation, localization, and loss beyond the free electron model," *Phys. Rev. B.*, vol. 72, 075405-1-11, 2005.
- [4] P. Berini, "Figures of merit for surface plasmon waveguides," *Opt. Express*, vol. 14, pp. 13030-13042, 2006.
- [5] J. A. Dionne, et al., "Plasmon slot waveguides: Towards chip-scale propagation with subwavelength-scale localization," *Phys. Rev. B*, vol. 73, pp. 035407-1-9, 2006.
- [6] I. V. Shadrivov, A. A. Sukhorukov, and Y. S. Kivshar, "Guided modes in negative-refractive-index waveguides," *Phys. Rev. E*, vol. 67, pp. 057602-1-4, 2003.
- [7] S. Foteinopoulou and J.-P. Vigneron, "Extended slow-light field enhancement in positive-index/negative-index heterostructures," *Phys. Rev. B*, vol. 88, pp. 195144-1-8, 2013.
- [8] S. I. Bozhevolnyi, et al., "Photonic bandgap structures for long-range surface-plasmon polaritons," *Opt. Comm.*, vol. 250, pp. 328-333, 2005.
- [9] A. Karalis, et al., "Surface-plasmon-assisted guiding of broadband slow and subwavelength light in air," *Phys. Rev. Lett.*, vol. 95, pp. 063901-1-4, 2005.
- [10] S. Foteinopoulou, et al., "Backward surface waves at photonic crystals," *Phys. Rev. B*, vol. 75, pp. 245116-1-6, 2007.
- [11] S. Foteinopoulou, et al., "Experimental verification of backward wave propagation at photonic crystal surfaces," *Appl. Phys. Lett.*, vol. 91, pp. 214102-1-3, 2007.
- [12] S. Foteinopoulou, et al., "Tailoring the properties of designer surface plasmons for subdiffraction light

- manipulation,” in *FiO 2008/LS XXIV/Plasmonics and Metamaterials, OSA Technical Digest*, paper MThC6, 2008.
- [13] A. I. Rahachou and I. V. Zozoulenko, “Wave-guiding properties of surface states in photonic crystals,” *J. Opt. Soc. Am. B*, vol. 23, pp. 1679-1683, 2006.
- [14] E. I. Smirnova, et al., “Simulation of photonic band gaps in metal rod lattices for microwave applications,” *J. Appl. Phys.*, vol. 91, pp. 960-968, 2002.
- [15] G. Veronis, “Finite-difference-frequency-domain technique,” *Encyclopedia of Nanotechnology*, Springer, pp. 843-852, 2012.
- [16] W. Shin, “3D Finite-Difference-Frequency-Domain Method for Plasmonics and Nanophotonics,” Ph.D. dissertation, Stanford U., 2013.
- [17] K. L. Tsakmakidis, et al., “Ultraslow waves on the nanoscale,” *Science*, vol. 358, pp. eaan5196-1-11, 2017.
- [18] K. L. Tsakmakidis, et al., “Completely stopped and dispersionless light in plasmonic waveguides,” *Phys. Rev. Lett.*, vol. 112, 167401-1-5, 2014.
- [19] C. Vandenbem, et al., “Guided waves in a bilayer film made of right- and left-handed materials,” presented at *Photonic Metamaterials: From Random to Periodic*, Grand Island, Bahamas, Paper WD5, 2006.
- [20] S. Foteinopoulou, “Electromagnetic energy accumulation in mesophotonic slow-light waveguides,” published in *19th International Conference on Transparent Optical Networks (ICTON)*, IEEE, pp. 1-4, 2017.
- [21] K. L. Tsakmakidis, A. D. Boardman, and O. Hess, “Trapped rainbow storage of light in metamaterials,” *Nature*, vol. 450, pp. 397-401, 2007.
- [22] T. F. Krauss, “Slow light in photonic crystal waveguides,” *J. of Physics D-Appl. Phys.*, vol. 40, pp. 2666-2670, 2007.
- [23] S. F. Mingaleev, A. E. Miroshnichenko, and Y. S. Kivshar, “Low-threshold bistability of slow light in photonic-crystal waveguides,” *Opt. Express*, vol. 15, pp. 12380-12385, 2007.
- [24] S. A. Schulz, et al., “Photonic crystal slow light waveguides in a kagome lattice,” *Opt. Lett.*, vol. 42, pp. 3243-3246, 2017.
- [25] A. Ambrosio, et al., “Selective excitation and imaging of ultraslow phonon polaritons in thin hexagonal boron nitride crystals,” *Light Science and Appl.*, vol. 7, pp. 27-1-9, 2018.
- [26] S. He, Y. He, and Y. Jin, “Revealing the truth about ‘trapped rainbow’ storage of light in metamaterials,” *Scientific Reports*, vol. 2, pp. 583-1-9, 2012.
- [27] A. Taflove, *Computational Electrodynamics: The Finite Difference Time-Domain Method*. Artech House, Boston, 1995.
- [28] A. Alu and N. Engheta, “Guided modes in a waveguide filled with a pair of single-negative (SNG), double-negative (DNG), and/or double-positive (DPS) layers,” *IEEE Trans. Microwave Theory Tech.*, vol. 52, pp. 199-210, 2004.
- [29] V. G. Veselago, “The electrodynamics of substances with simultaneously negative ϵ and μ ,” *Sov. Phys. Usp.*, 10, 509, 1968.
- [30] J. C. Knight, “Photonic crystal fibers,” *Nature*, vol. 424, pp. 847-851, 2003.
- [31] S. Foteinopoulou, “Frequency-domain versus time-domain analysis of slow-light mesophotonic waveguides: Theoretical insights for practically realizable devices,” *2018 International ACES Symposium*, Denver, CO, pp. 1-2, 2018.
- [32] A. Otto, “Excitation of nonradiative surface plasma waves in silver by the method of frustrated total reflection,” *Z. Phys.*, vol. 216, 398-410, Aug. 1968.
- [33] S. Foteinopoulou and C. M. Soukoulis, “Negative refraction and left-handed behavior in two-dimensional photonic crystals,” *Phys. Rev. B*, vol. 67, 235107-1-5, 2003.
- [34] J. Peatross, S. A. Glasgow, and M. Ware, “Average energy flow of optical pulses in dispersive media,” *Phys. Rev. Lett.*, vol. 84, pp. 2370-2373, 2000.



Stavroula Foteinopoulou is a Research Professor with the ECE Dept. of the U. of New Mexico. She received her Ph.D. in Condensed Matter Physics from Iowa State U. and has held post-doctoral positions in U. of Namur (Belgium) as well as the Institute of Electronic Structure and Laser (IESL) of FORTH (Greece). She was a Lecturer at the U. of Exeter (UK) until 2014 prior to joining the U. of New Mexico. Her research in theoretical/computational photonics focuses on conceiving new photonic platforms for unconventional light control across the EM spectrum. She has authored more than 30 journal publications and conference papers, which have attracted to-date more than 2800 citations (source google scholar). She also holds one US patent. Stavroula is serving as an Associate Editor for the OSA Optical Materials Express (OMEX) Journal, as well as for the Journal of the European Optical Society: Rapid Publications (JEOS-RP). She is also a Chair of the annual SPIE Conference Active Photonic Platforms.